# Automated Bow Shock and Magnetopause Boundary Classification At Saturn Using Statistics of Magnetic Fields and Particle Flux

I Cheng[1], Nick Achilleos[2], and Patrick Guio[2]

[1]UCL
[2]University College London

November 21, 2022

**Abstract**

Statistical studies of the properties of different plasma regions, such as the magnetosheath and outer magnetosphere found near the boundaries of planetary magnetospheres, require knowledge of boundary (bow shock and magnetopause) crossings for purposes of classification. These are commonly detected by visual inspection of the magnetic field and / or particle data sampled by the relevant spacecraft. Automation of this type of activity would thus improve the efficiency of boundary and region studies, which benefit from large crossing datasets, and could also have implications for future development of onboard data-processing protocols in the pre-downlink stage. The Cassini mission at Saturn (2004-2017) provided an invaluable dataset for testing the viability of automated boundary classification. The training dataset consists of BS and MP crossings for the time period 2004 to 2016 (Jackman et al. (2019)). We have employed a series of techniques which involve pre-processing the calibrated magnetometer data, unsupervised training of a LSTM recurrent neural network on magnetometer data to filter magnetosheath regions where crossings are most likely to be found, isolating large rotations in magnetic field using minimum variance analysis (MVA), feature engineering such as magnetic field strength ratio either side of the field rotation to form a 'feature vector' for each candidate, and finally applying a gradient-boosting decision-tree-based algorithm to predict the probability that a given interval of data contains the signature of a bow shock (BS), a magnetopause (MP), or None (not a boundary crossing). The resulting model performs better on bow shock events, with a precision (fraction of true events in the retrieved sample) and recall (fraction of the total true events which were retrieved) of ˜86% and ˜90% respectively, as compared to ˜50% and ˜68% for the MP. The ongoing work focuses on augmenting the feature space for improved classification of MP, based on a magnetic pressure model of MP crossings derived using a local pressure balance condition (e.g. Pilkington et al. 2015) and using the distinct energetic particle flux changes across the MP in MIMI data (e.g. Liou et al. 2021). We expect that these promising new features will help us to better constrain the retrieval of candidate events which are true MP crossings.

# Automated Bow Shock and Magnetopause Boundary Detection With Cassini Using Threshold and Deep Learning Methods

I Cheng [1], Nick Achilleos [1], Patrick Guio [2]
[1] Department of Physics and Astronomy, University College London, London, UK; [2] Department of Physics and Technology, Arctic University of Norway, Tromso, Norway
Email: i.cheng.19@ucl.ac.uk | Poster: https://bit.ly/3lEzdde | **Video**: **https://youtu.be/eSLz3rlwvsk**

## Motivation

**Manually searching by eye for bow shock (BS) and magnetopause (MP) boundaries in spacecraft data is:** Time consuming, prone to human **error**, requires **expertise.**

**Automation will allow:** **Reproducibility, discovery** potential in unlabeled data, **reusability** in existing and future planetary missions.

**BS and MP boundaries contain interesting physics such as:**
**Morphology** in which the 3-d shape and size of the magnetosphere (SP), MP and BS affect plasma flows in the magnetosheath (SH). **Dynamics** like current systems, magnetic reconnection, shock physics and plasma energization. **Instabilities** like R-T waves, K-H waves, Kinetic waves, Mirror mode waves, Helical instability, Heat-flux driven instability, Modified two-stream instability, Lower-hybrid drift Instability [1, 2].

## BS and MP Crossing Signatures

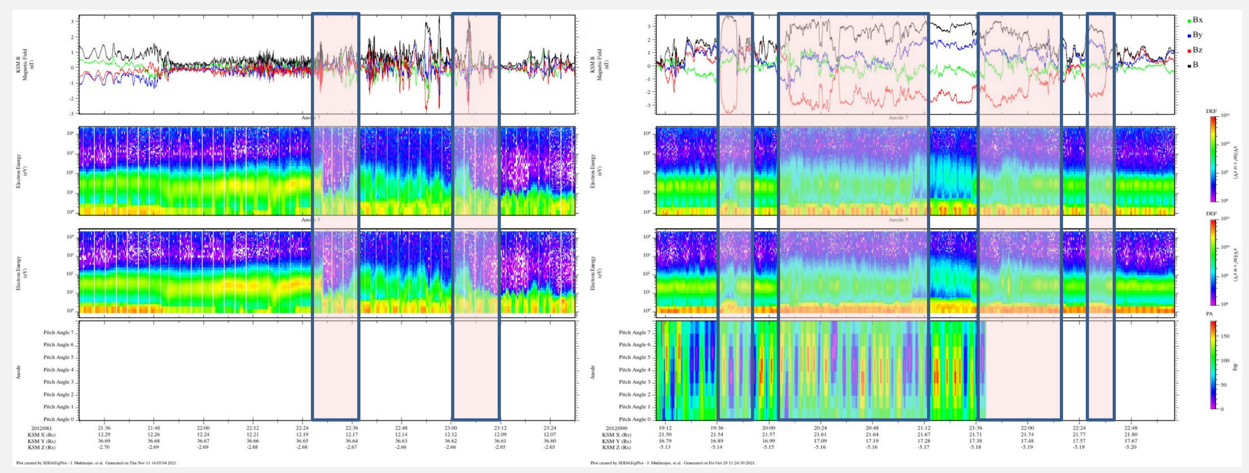

Fig. 1: MAG[13] Data and CAPS[14] ELS Anode 5 and 7 with pitch angle information for intervals of example BS (left) and MP (right) crossings. Adapted from *cassinimag.space.swri.edu.*

**Typical signatures of BS crossings include (Fig 1 left):**

- **Magnetic field:** The SW magnetic field is weaker (typ. <1nT) than in the SH; often with magnetic overshoot feature due to ion reflection and gyration [5].
- **Plasma:** The SH plasma is denser and hotter than solar wind plasma due to conversion of kinetic to thermal energy by the BS.

**Typical signatures of MP crossings include (Fig 1 right):**

- **Magnetic field:** The $B_z$ component is usually negative (southward) inside the low-latitude magnetosphere, whereas the SH $B_z$ is typically close to zero but highly variable. **Plasma:** The magnetospheric plasma is less dense and hotter than SH plasma.

For both boundaries, the field fluctuations typically increase in the SH due to turbulence.

## Ground Truth

The BS and MP ground truth catalogue used contains over 2100 MP crossings, and over 1200 BS crossings [3,4]. They are recorded as single timestamps.

## Define the problem

To simplify the problem, binary classification is performed (Fig 2).


Fig. 2: Schematic of the problem. Question: Is there a BS or MP crossing or not?

## Pipeline

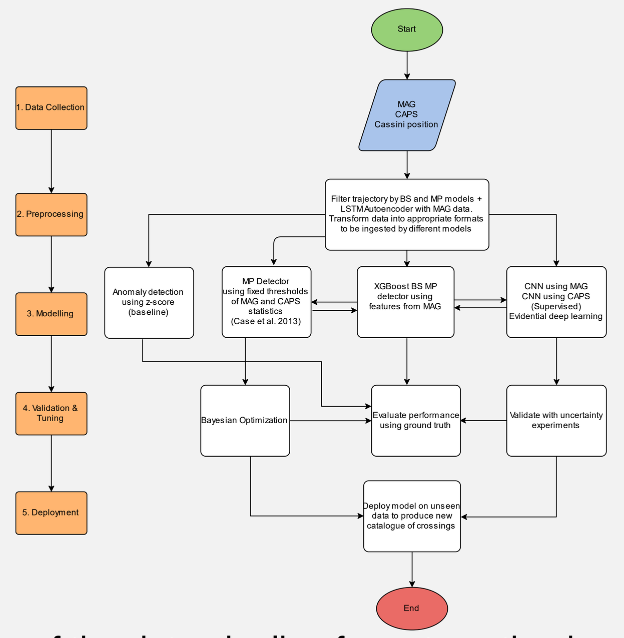

Fig. 3: Five stages of the data pipeline for automating boundary detection: 1) Data collection. 2) Pre-processing. 3) Modelling the data with different methods. 4) Validating and tunning the algorithm. 5) Deployment on new data.

## Preprocessing

Data collection is complete thanks to Cassini. The next step (Fig. 3) is preprocessing the data for automated BS/ MP boundary detection.

1. To reduce the search scope, sections of Cassini's orbits were pre-selected (Fig 4) based on expected BS and MP locations using empirical models. This filtering reduced the amount of data to $4.2 \times 10^6$ minutes (between 2004- 2016).

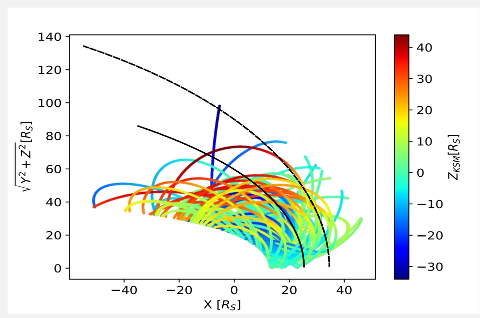

Fig. 4: Orbit selection based on expected BS and MP locations and crossings catalogue.

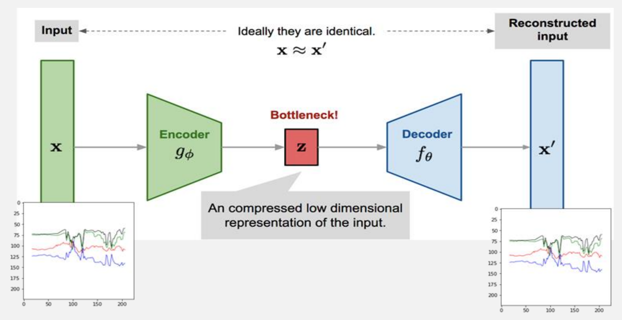

Fig. 5: Schematic of LSTM autoencoder used for filtering intervals of magnetic field data with abrupt changes.

2. To further reduce the scope, a LSTM autoencoder (Fig. 5) was employed for unsupervised outlier detection. Over-parameterized neural networks (NN) have been shown to prioritize learning simple patterns that generalize across data samples [6]. This property was well-suited for filtering intervals with sudden changes in field which typically signal BS and MP boundary crossings.

## Modelling

Two methods are compared in this poster:

1. **Threshold method** [7] : MAG and CAPS parameter values were computed using two sliding windows of length 30 minutes with a fixed gap of 8 minutes in between (shown by the red squares in Fig. 6). This method is easily explainable due to the physical meaning of the parameters such as fluctuations in the field. A positive detection occurs when a fixed threshold is exceeded in all the parameters.
2. **Deep learning with convolutional neural network (CNN)** [8] : Motivated by the ability of human eyes to recognize BS and MP features from multi-instrument plots (like Fig 1). A CNN automatically creates discriminative features from the input image in order to output the correct class label using labelled training data. A ResNet architecture was used due to the benefits of skip-connections [9] , where inputs are directly added to the output of a layer (see Fig. 7 right).

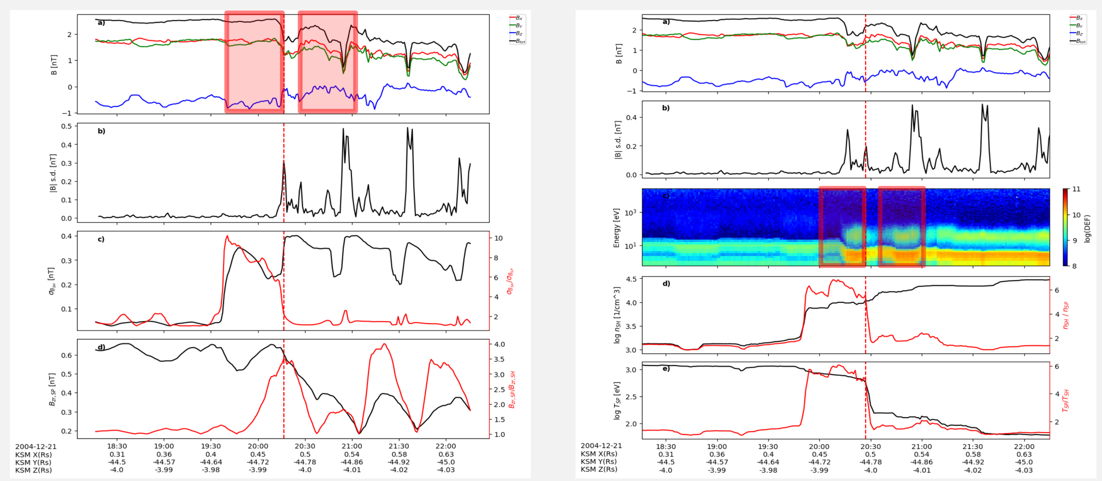

Fig. 6: **MAG threshold method** (left) to detect MP using four magnetic field parameters: 1) B standard deviation in SH, 2) ratio of B standard deviation between SH and SP, 3) North-south/ radial component of B in SP, 4) ratio of Bz or Br between SP and SH. Thresholds optimised using Bayesian optimisation. **CAPS threshold method** (right) to detect MP using four density and temperature parameters: 1) log density in SH, 2) ratio of density between SH and SP, 3) log temperature in SP, 4) ratio of temperature between SP and SH.

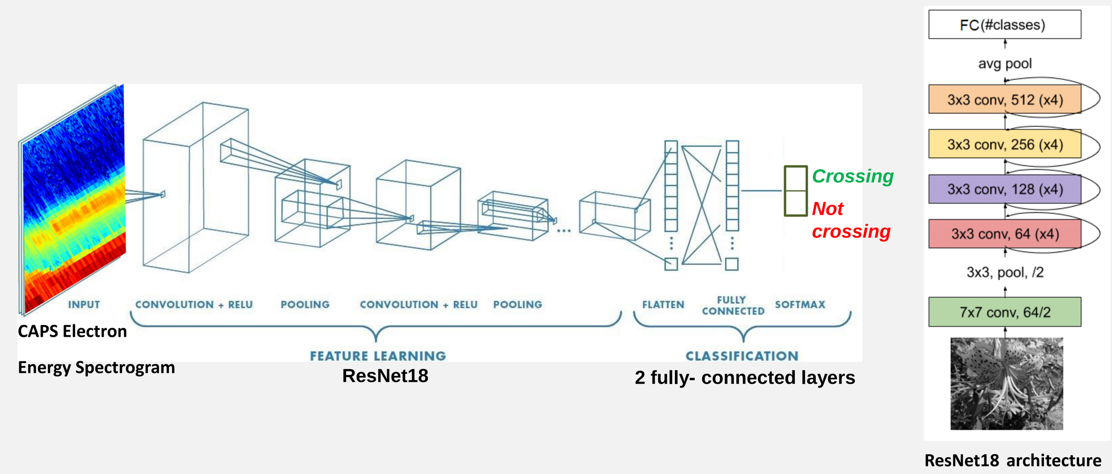


Fig. 7: Schematic of CNN classifier (left) showing how an input image of CAPS electron energy spectrogram is passed through the convolutional layers, generating deeper and deeper feature maps, eventually flattened to be passed through a fully connected network for classification giving output 'crossing' or 'notCrossing'. Schematic of ResNet architecture (right) used in the feature learning part with arrows showing skip-connections.

## Validating and Tunning

To tune the threshold method, the best parameter thresholds were found using Bayesian optimization[10] to maximize F1 score (a metric of both (1) how many of the ground truth are detected (recall) and (2) how many of these detections are true crossings (precision)). A tolerance of ±60 minutes from a ground truth crossing was defined as correct.

To validate the CNN, Grad-CAM[11] was used to visualize what the network was using to make its predictions (see Fig. 8).

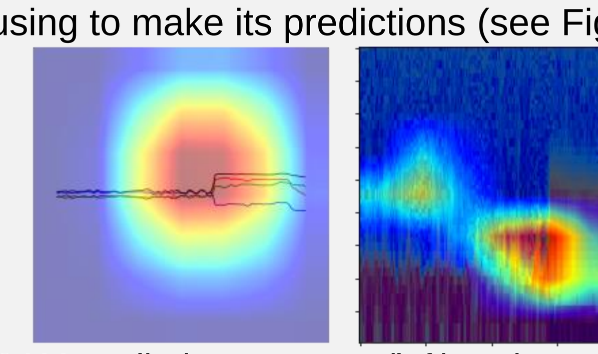

Fig. 8: Grad-CAM applied to *cnn-mag* (left) and *cnn-caps* (right). The heatmap shows regions which are most discriminative for the output class (red regions highlight the most important pixels). Both models highlight the region with discontinuity as most important, which is what our eyes would focus on too for deciding between crossing or not.

Additional checks were implemented to 'screen' for genuine MP crossings as these tended to be the most difficult to detect especially in the dusk sector. These included: Angular deviation between MP model, TD and MVA normal, power spectra of parallel and perpendicular magnetic field, candidate crossing location on magnetic pressure map, predicted plasma beta based on pressure balance assumption, fluctuations of normal component of magnetic field from MVA, the ratio $B_R/B$ at low latitudes assuming closed MP.

## Results

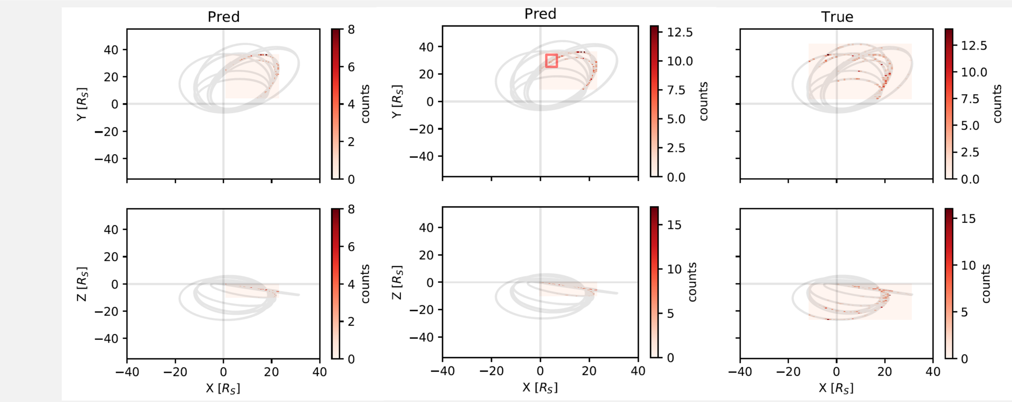

Fig. 9: 2d histogram of crossing prediction locations in 2012 by *thresh-caps* (left), *cnn-caps (middle)*, and current ground truth (right). There is a region of crossing predictions (marked by red square) in *cnn-caps* which is not seen in *thresh-caps* or ground truth.

| | precision | recall | f1-score | support |
|---|---|---|---|---|
| 0_notCrossing | 0.995 | 0.986 | 0.990 | 2622 |
| 1_crossing | 0.910 | 0.967 | 0.937 | 395 |
| accuracy | | | 0.983 | 3017 |
| macro avg | 0.952 | 0.976 | 0.964 | 3017 |
| weighted avg | 0.984 | 0.983 | 0.983 | 3017 |

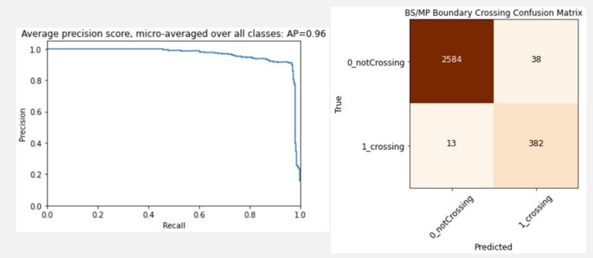


Fig. 10: Error analysis of the *cnn-caps* and post-correction performance for test year 2012, with all metrics exceeding 90%.

**Error analysis of *cnn-caps* misclassifications revealed:**

- 48.5% were MP
- 26.5% were BS
- 12.2% occurred in SH
- 11.7% occurred in SP
- 1.0 % occurred in SW
- Causes include missing BS and MP in ground truth and intervals with no CAPS data but exists in ground truth using MAG-based crossings.

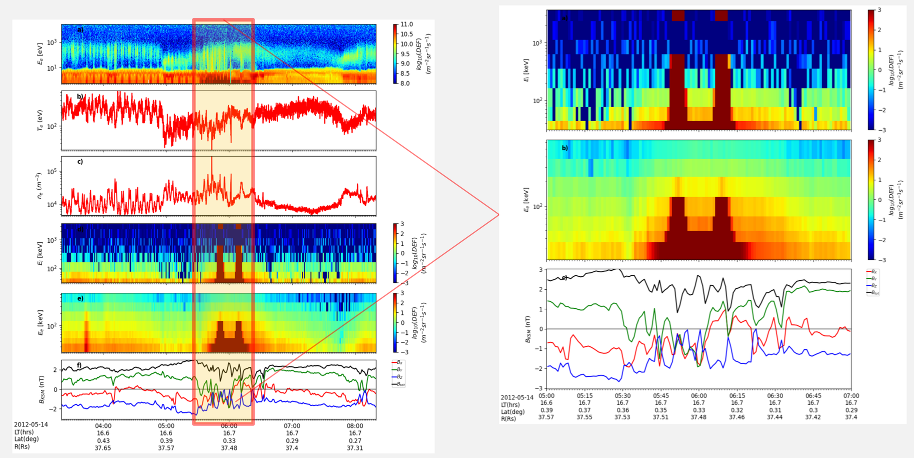

Fig. 11: A 'crossing' event flagged by CNN method not previously recorded. This event situated on the dusk flank near the equator is similar to the K-H vortex encounter discussed in Masters et al. (2010) [12].

## Conclusion and Future Work

1. It is possible to automate the detection of BS and MP crossings using magnetic field data and electron energy spectrogram as demonstrated with Cassini data at Saturn.
2. Two methods were compared: Threshold (Fig. 6), CNN (Fig. 7).
3. Based on 2012 test data and the latest BS and MP catalogue at Saturn, the CNN approach outperforms the threshold approach (Fig. 9 and Fig. 10).
4. Both are lightweight and effective tools for large scale boundary surveys of spacecraft data and speed up catalogue creation.
5. Potential case studies from shortlisted events (e.g., Fig. 11).

## References

[1] Baumjohann, W., & Treumann, R. A. (1996). Basic Space Plasma Physics. *Imperial College Press*.
[2] Treumann, R. A., & Baumjohann, W. (1997). Advanced Space Plasma Physics. *Imperial College Press*.
[3] Jackman et al. (2019). Survey of Saturn's Magnetopause and Bow Shock Positions Over the Entire Cassini Mission: Boundary Statistical Properties and Exploration of Associated Upstream Conditions. *JGR Space Physics.*
[4] Pilkington et al. (2015). Asymmetries observed in Saturn's magnetopause geometry, *GRL.*
[5] Gosling and Robson (1985). Ion Reflection, Gyration, and Dissipation at Supercritical Shocks. *Geophys*.
[6] Rahaman et al. (2019). On the spectral bias of neural network.
[7] Case and Wild (2013). The location of the Earth's magnetopause: A comparison of modeled position and in situ Cluster data. *JGR Space Physics*.
[8] Lecun et al. (1998). Gradient-based learning applied to document recognition. *Proceedings of the IEEE*.
[9] He et al. (2015). Deep Residual Learning for Image Recognition.
[10] Balandat et al. (2020). BoTorch: A Framework for Efficient Monte-Carlo Bayesian Optimization. *NIPS*.
[11] Selvaraju et al. (2019). Grad-CAM: Visual Explanations from Deep Networks via Gradient-based Localization
[12] Masters et al. (2010). Cassini observations of a Kelvin-Helmholtz vortex in Saturn's outer magnetosphere. *JGR*.
[13] Dougherty et al. (2004). The Cassini magnetic field investigation. *Space Science Reviews*.
[14] Young et al. (2004). Cassini plasma spectrometer investigation. *Space Science Reviews.*